

Automated hyperemia analysis software: reliability and reproducibility in healthy subjects

Tsuyoshi Yoneda · Tamaki Sumi · Ayako Takahashi ·
Yasuhiro Hoshikawa · Masahiko Kobayashi ·
Atsuki Fukushima

Received: 7 March 2011 / Accepted: 5 October 2011 / Published online: 1 December 2011
© Japanese Ophthalmological Society 2011

Abstract

Purpose To evaluate the reliability and reproducibility of automated software to analyze human bulbar hyperemia.

Methods We enrolled 89 healthy volunteers in this study. A slit lamp was used to take pictures of the conjunctiva on the temporal side of each subject's right eye. Photographic conditions were standardized by using a single photographer. Images were transferred to software for automatic pixel value calculation in the green channel of the region of interest (ROI). We investigated optimal ROI size, mean ROI pixel frequency, percentage ROI blood vessel coverage, and data reproducibility. We also used this software to evaluate bimatoprost-induced hyperemia and hyperemia in allergic conjunctival diseases.

Results The optimal ROI was found to be 400 vertical pixels by 300 horizontal pixels. Mean ROI pixel frequency was 5305 and % coverage was 4.4%. We confirmed the reproducibility of the analysis by comparing two images ($r^2 = 0.7$, $P < 0.0001$). Percentage blood vessel coverage increased in images of bimatoprost-induced hyperemia and hyperemia in allergic conjunctival diseases compared to the data from healthy volunteers.

Conclusions The software was simple to use and provided reproducible data. We established standard settings for the operation of the software. The use of our software will improve hyperemia evaluation, which is presently done using nonquantitative methods.

Keywords Conjunctiva · Hyperemia · Image analysis · Software

Introduction

Conjunctival hyperemia is observed in a variety of ocular inflammatory conditions, including ocular surface inflammation [1] (corneal infection and allergic conjunctivitis) and intraocular inflammations (uveitis and scleritis) [2]. Conjunctival hyperemia also indicates the severity of ocular inflammation [3]. Thus, evaluating conjunctival hyperemia is critically important for the treatment of patients with ocular inflammation.

As described elsewhere [4], clinical evaluation of conjunctival hyperemia is subjective, and relies on grading scales such as the McMonnies/Chapman-Davies scale [5], the Institute for Eye Research scale [6], the Efron scale [7], and a validated bulbar redness scale [8]. The grades generally range from zero to four or five. The scoring scales in these systems increment in single units. A clinician grading an eye with bulbar hyperemia halfway between grade 0 and grade 1 on the Efron scale will give a grade of 0.5. Thus, a weakness of this method is that it cannot provide a continuous linear quantitative evaluation.

To overcome the limitations of current scoring methods for its quantitative evaluation, we examined the severity of conjunctival hyperemia using image analysis in guinea pigs, where hyperemia was observed in histamine-induced [9] or antigen-induced conjunctivitis [10]. We demonstrated that conjunctival hyperemia can be quantitatively evaluated by measuring the percentage pixel coverage in images of the region of interest (ROI). This particular method has never been applied to conjunctival hyperemia evaluation in humans, so we aimed to create the necessary

T. Yoneda · T. Sumi · A. Takahashi · A. Fukushima (✉)
Department of Ophthalmology and Visual Science, Kochi
Medical School, Kohasu, Oko-cho, Nankoku 783-8505, Japan
e-mail: fukushima@kochi-u.ac.jp

Y. Hoshikawa · M. Kobayashi
NIDEK Co., Ltd., Gamagori, Japan

automated software to analyze conjunctival hyperemia and to examine the applicability of our software for conjunctival hyperemia evaluation in humans.

Materials and methods

Participants

We enrolled 89 healthy volunteers for this study. Subjects had no history of ocular disease other than refractive errors. Participant ages ranged from 20 to 46 years (mean \pm standard deviation 25.4 ± 4.2 years). Contact lens users were excluded from this study. The study was approved by the Ethical Review Board of Kochi Medical School, and each participant provided written informed consent after receiving a detailed description of the planned procedure and the aim of the study. Three participants received a single treatment of bimatoprost eye drops OD only. These three participants also provided informed consent with respect to possible side effects of the bimatoprost eye drops. In addition to the healthy volunteers, three patients with allergic conjunctival diseases were also enrolled. Two of them were diagnosed as having perennial allergic conjunctivitis, while the other was diagnosed as having vernal keratoconjunctivitis.

Image acquisition procedure

We photographed the conjunctiva on the temporal side of each participant's right eye using a slit lamp (model SL-D7; Topcon, Tokyo, Japan). Photographs were taken twice, with an interval of 5 s between them, in each participant. The slit width was set at 20 mm and the objective magnification was set at $\times 10$. The angle between the lamp and microscope arm was set at 30° . Camera light was adjusted to level two. The diffuser was removed and, to avoid saturation caused by background light and observation light, we turned off the observation lamp during photography. Photographs were stored as JPEG images with a resolution of 2000×1312 pixels. These images were processed using the newly developed software. Photographs were taken of participants treated with bimatoprost, both before treatment and 12 h after treatment.

Software algorithm

The shape of the ROI was selected as a rectangle (Fig. 1, surrounded by a blue line). The data for the ROI is shown in the middle left portion (closed red circle). We extracted blood vessel images by setting RGB threshold values for the ROI analysis (Fig. 1, upper left, surrounded by a dotted red circle). RGB threshold settings are also shown in the middle left portion of Fig. 1 (surrounded by a dotted red

circle). The optimum conditions for blood vessel visualization were to set the red and blue values to zero, which allowed the threshold values of the green channel to be modified. The threshold value of the green channel was set and pixel frequencies for the conjunctival vessels were automatically calculated, as shown in Fig. 1 (middle left, surrounded by a closed red square). The fractal dimension of the blood vessels was measured using the box counting method [11], as shown in Fig. 1 (lower left, surrounded by a dotted red square).

Determination of ROI

Using the hyperemia analysis software, we evaluated the proportion of blood vessels in the conjunctiva. Initially, a broad area of the conjunctiva was selected as the ROI. However, because the eyeball is spherical, we found that the edge of the ROI was too dark for accurate evaluation. We then selected a standard ROI which can be evaluated reliably. An ROI containing 500 vertical pixels and 400 horizontal pixels was selected. Figure 2a (surrounded by a dotted red line) shows that the vessels were not visualized in the lower portions of the ROI, but vessel images were extracted even though no vessels were present in the upper left region of the ROI (surrounded by a solid red line). Based on these two results, we modified the ROI to 400 vertical pixels and 300 horizontal pixels. Figure 2b shows that the visualization of the vessels was satisfactory for an ROI with these dimensions.

Pixel coverage

The percentage pixel coverage was calculated by dividing the frequency of blood vessel pixels by the total pixel frequency, i.e., 300×400 pixels.

Statistical analysis

Reproducibility was evaluated using the Pearson's moment correlation coefficient (Pearson's r) and the intraclass correlation coefficient. Normality of pixel value distributions in healthy volunteers was checked using the Kolmogorov–Smirnov test. The percentage pixel coverage in bimatoprost-treated participants was compared using the Wilcoxon signed-rank test.

Results

Data reproducibility

We evaluated ROI suitability by testing 89 study volunteers who had no ocular diseases other than refractive

Fig. 1 Image appearance with the software. RGB channel threshold selections are shown in the upper left of this panel (dotted red circle). ROI information and pixel frequencies are shown in the middle left of the panel (closed red circle). Pixel frequencies for the conjunctival vessels were automatically calculated for the middle left of the panel (closed red square). Fractal dimensions are shown in the lower left of this panel (dotted red square)

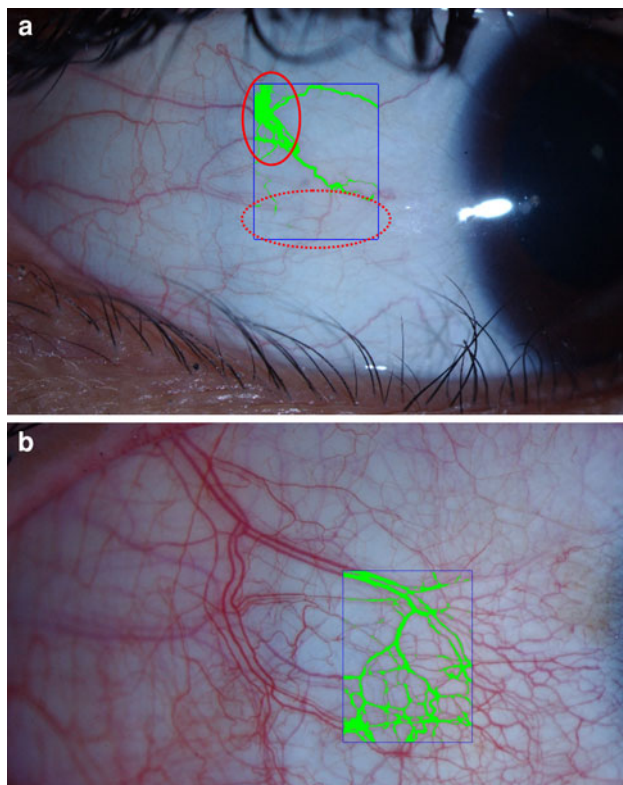
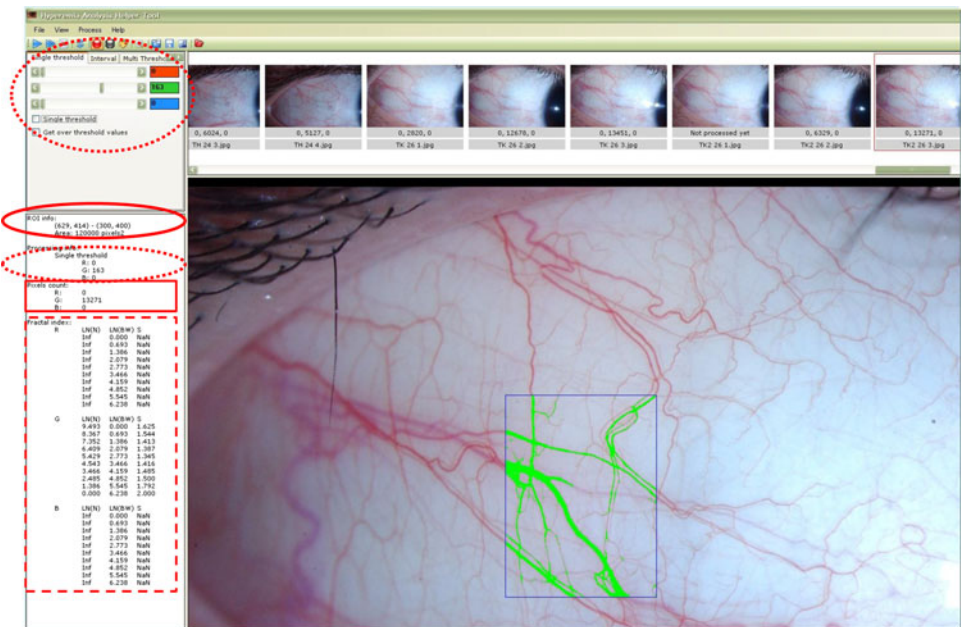


Fig. 2 ROI size determination. **a** ROI was set as 500 vertical pixels and 400 horizontal pixels. Vessels were not visualized in the lower ROI region (dotted line). Vessel images were visualized when no vessels were present in the upper left ROI region (solid line). **b** ROI was set to be 400 vertical pixels and 300 horizontal pixels. Visualization of vessels was satisfactory for this ROI size compared to **a**

abnormalities. Two slit photographs were taken of the temporal portion of the conjunctiva with a 5 s interval between them. The photographs were transferred to a

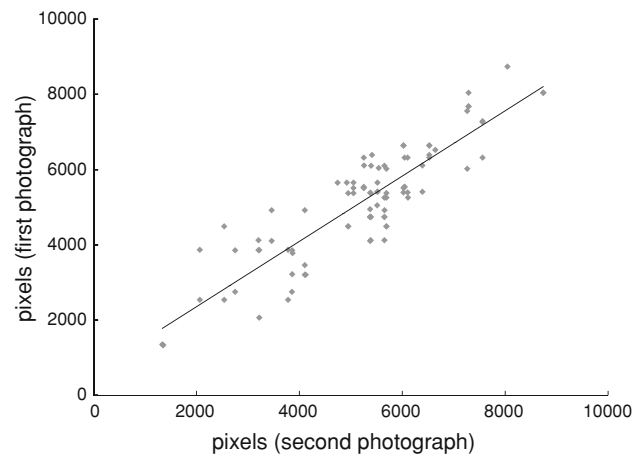


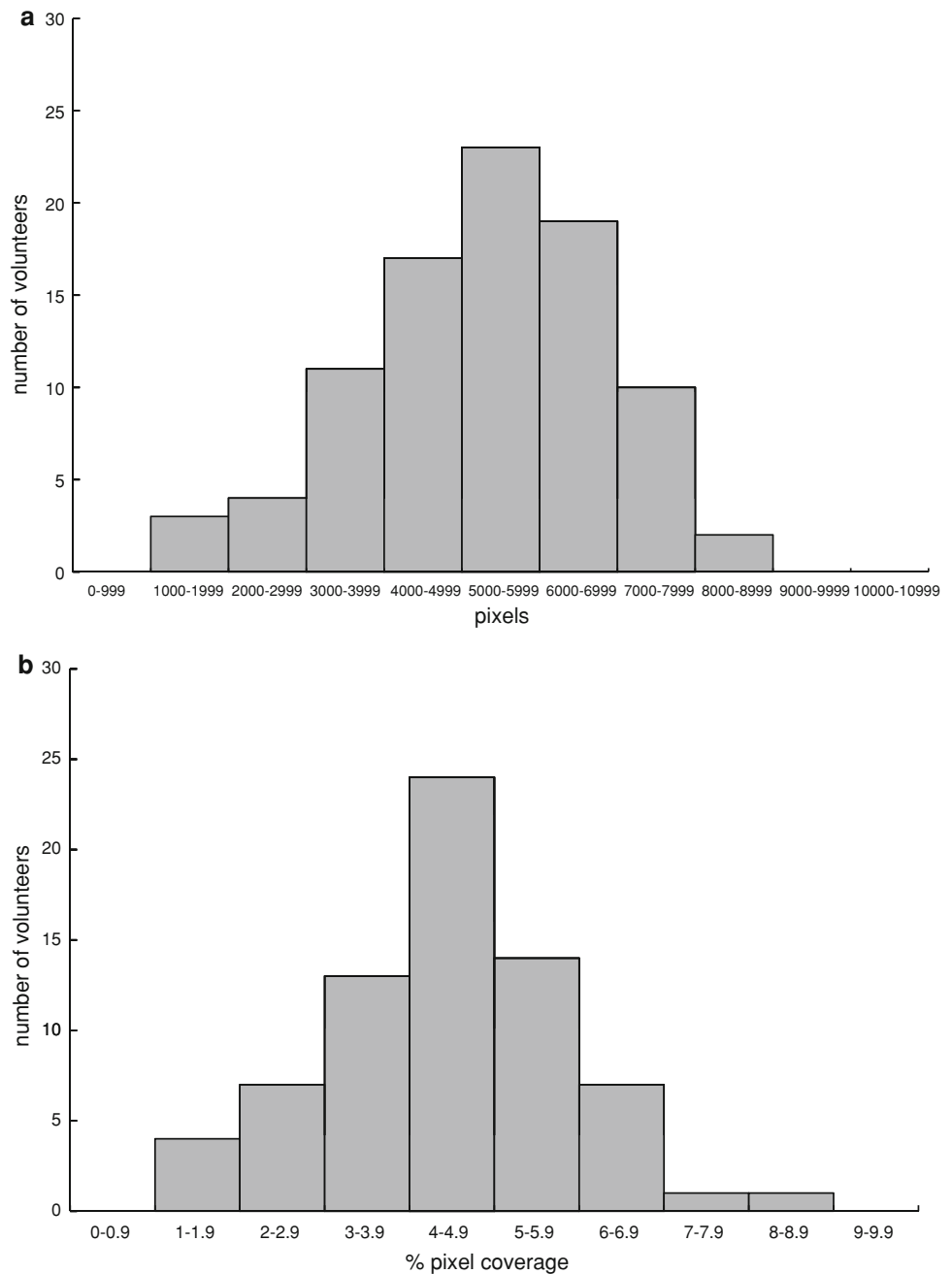
Fig. 3 Reproducibility of the data. Slit photographs of the temporal portions of the conjunctiva of 89 volunteers were taken twice with an interval of 5 s between them. The images were transferred to the software and two data from each volunteer were plotted. Result: $y = 0.8682x + 618.68$; $r^2 = 0.79$; x -axis indicates the pixel value of the second photograph and y -axis indicates that of the first photograph. Pearson's moment correlation coefficient: $P < 0.0001$; interclass correlation coefficient: $P < 0.0001$

computer and analyzed with the software. Figure 3 shows that analytical reproducibility was confirmed ($r^2 = 0.79$) ($P < 0.0001$).

Evaluation of hyperemia in healthy volunteers

We determined the mean pixel frequencies of the conjunctival blood vessels for the 89 volunteers. Figure 4a shows that the mean was 5305 pixels (Fig. 4a). Pixel values varied among the participants to the extent that the minimum and maximum values differed by a factor of ten. We

Fig. 4 Evaluation of hyperemia in healthy volunteers. **a** Distribution of pixel values in 89 volunteers. X-axis indicates pixel values and y-axis indicates the number of volunteers (average 5305). The normality of the distribution was confirmed by the Kolmogorov–Smirnov test ($P > 0.05$). **b** Percent pixel coverage of vessels in the ROI. X-axis indicates % pixel coverage and y-axis indicates the number of volunteers (average 4.4%). The normality of the distribution was confirmed by the Kolmogorov–Smirnov test ($P > 0.05$)



also evaluated conjunctival hyperemia by measuring the percentage pixel coverage, and found that the mean percentage was 4.4% (Fig. 4b). The normality of distribution was confirmed using the Kolmogorov–Smirnov test (Fig. 4a, b, $P > 0.05$).

Hyperemia induction using bimatoprost

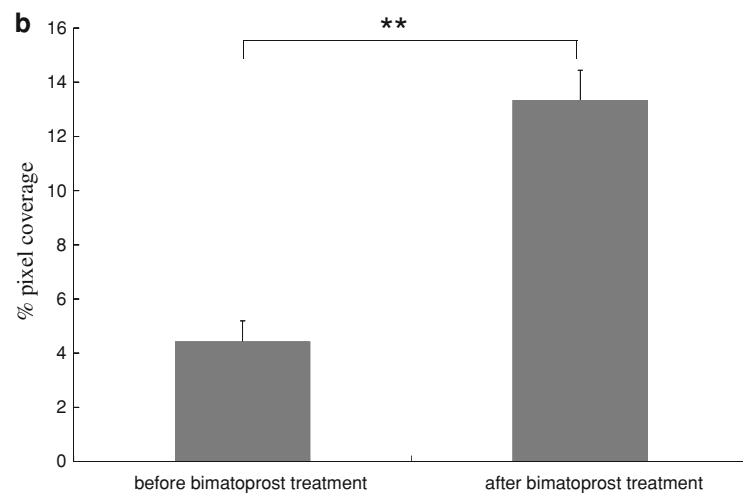
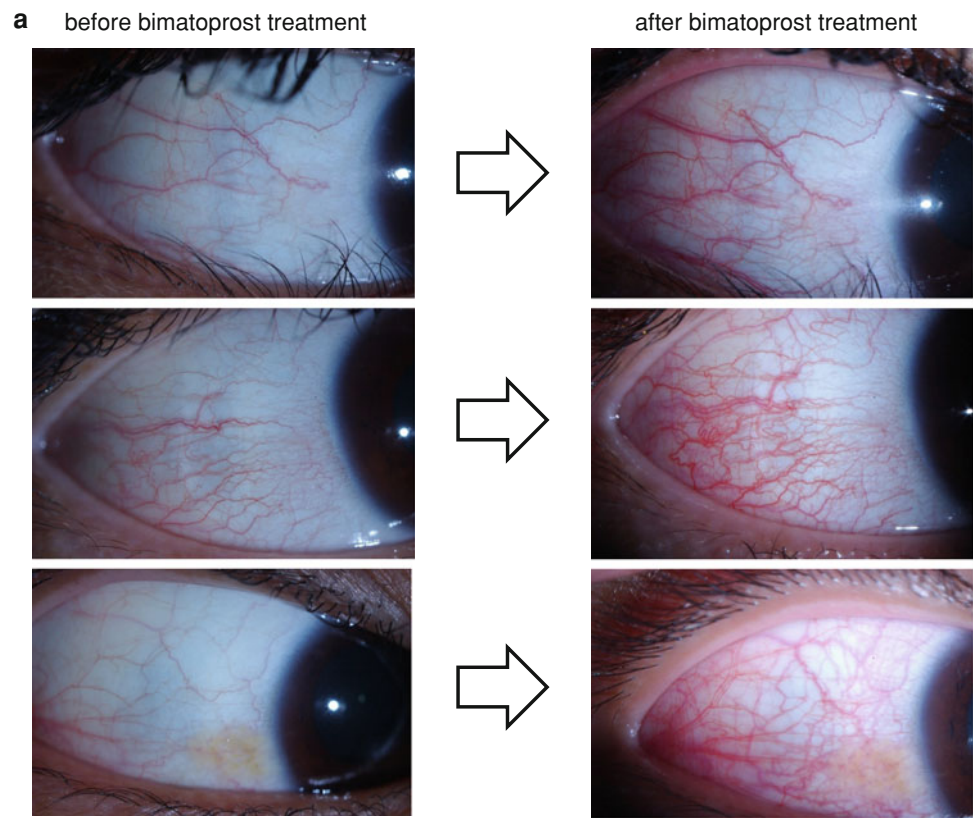
All three participants receiving bimatoprost eye drops OD presented clinical hyperemia 12 h after treatment (Fig. 5a). Hyperemia disappeared spontaneously after a few days.

The mean blood vessel percentage coverage in the ROIs of the three participants increased significantly from 4.4 to 13.4% ($P < 0.001$) (Fig. 5b).

Evaluation of hyperemia in patients with allergic conjunctivitis

Hyperemia was noted in all three patients with allergic conjunctival diseases (Fig. 6). The pixel values and blood vessel percentage coverages in the ROIs of the three participants were 28691 pixels and 23.9% (Fig. 6a), 30336

Fig. 5 Hyperemia induced by bimatoprost. **a** Photographs of the conjunctiva. Photographs were taken of three participants who received bimatoprost eye drops OD either before (*left column*) or 12 h after (*right column*) treatment. **b** Average % coverage in the ROI. Average coverage was 4.4% before and 13.4% after treatment. $**P < 0.001$, Wilcoxon signed-rank test



pixels and 25.3% (Fig. 6b), and 31801 pixels and 26.5% (Fig. 6c).

Discussion

Several authors have reported the application of computerized image analysis techniques for grading anterior eye characteristics. As previously described by Wolffsohn [12], bulbar hyperemia has been graded by a combination of thresholding [13–17], edge detection [14, 18, 19],

smoothing [13, 14, 18, 20], color extraction [13, 15, 17, 20], morphometry and densitometry [21]. However, these experimental methods were highly complex and have not been routinely used in a clinical setting. Several reports indicate the possible application of software to automate conjunctival hyperemia evaluation [14, 15, 18, 20]. These methods are not widely used in a clinical setting, probably due to difficulties with accessibility, operation, maintenance, and development costs. For example, Schulze and Fieguth attempted to establish an automatic image analysis technique, but the binary processing of images and fractal

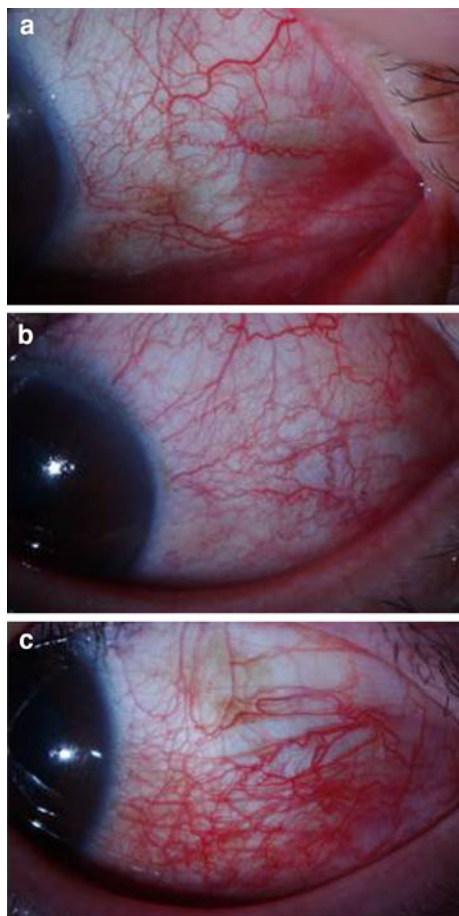


Fig. 6 Hyperemia in patients with allergic conjunctival diseases. Photographs of the conjunctiva with allergic conjunctival diseases. Two patients were diagnosed as having perennial allergic conjunctivitis (**a**, **b**), while one patient (**c**) was diagnosed as having vernal keratoconjunctivitis

analysis by edge detection were too complicated [4, 8, 13]. Therefore, we aimed to develop an automated system that could easily facilitate conjunctival hyperemia analysis and numerical data presentation. Unlike previous reports, our software makes analysis simple; images from the pictures taken by the slit lamp can be analyzed promptly.

Ideally, the evaluation of hyperemia should assess the entire area of the bulbar conjunctiva. Initially, we selected a broad area of the conjunctiva for evaluation. However, we found that the spherical shape of the eyeball meant that blood vessel images were typically either overextracted or underextracted. Therefore, we determined the optimum ROI (400 vertical pixels \times 300 horizontal pixels) for extracting blood vessel images in both a reliable and a reproducible manner. Data from 89 volunteers confirmed the reliability and reproducibility. To ensure standardized conditions, all photographs were taken by a single photographer. Because we had difficulties processing photographs from other institutes where photographic conditions were different, this proved a critical parameter in the

proper evaluation of conjunctival hyperemia. A previous researcher [13] observed that sampling methods are a source of confusion when clinicians are not from a single institution. To overcome this issue, the software requires an application to compensate for variable photographic conditions.

We also used our software to investigate hyperemia induced by eye drops containing bimatoprost, although the sample size was small. Three of the volunteers enrolled in this study exhibited an approximately threefold increase in vasculature. Additionally, we evaluated the degree of hyperemia in patients with allergic conjunctival diseases. Compared to the data from healthy volunteers (Fig. 4), pixel values and blood vessel percentage coverages in the ROIs of these three participants were approximately six-fold higher. These small studies show that our software might be applicable for the evaluation of moderate cases of conjunctival hyperemia as well. Researchers have reported that the correlation between computer image analysis and clinician grading was nonlinear, with a higher degree of discrepancy for higher grades of bulbar hyperemia [12, 14, 22]. This issue requires further investigation.

There are several points to be considered. One is how to discriminate between conjunctival hyperemia and other findings, such as pigmentation, nevus, and calcification. The other is how to determine the origin of the hyperemia (conjunctiva, episclera, or sclera). At present, it is not possible to achieve these two aims. The fractal dimension provides an indication of the complexity of the blood vessel distribution [4]. Thus, as the fractal dimension increases, the area of conjunctival hyperemia also increases. Because we did not analyze the fractal dimension data in this study, it will be necessary to evaluate the relationship between pixel values and fractal dimension in the analysis as a next step. This fractal dimension analysis may hint at some ways to achieve the two aims discussed above.

In conclusion, we developed a software package for conjunctival hyperemia evaluation. Our software is simple to operate and provides reliable and reproducible data. However, the software has limitations, because the ROI is restricted and the analysis is constrained by photographic conditions. To overcome these issues, we are conducting multicenter trials to collect hyperemia images.

References

- Alexander KL. Some inflammations of the external eye and adnexa. *J Am Optom Assoc.* 1980;51:142–7.
- van der Woerd A. Management of intraocular inflammatory disease. *Clin Tech Small Anim Pract.* 2001;16:58–61.
- Janssens M. Efficacy of levocabastine in conjunctival provocation studies. *Doc Ophthalmol.* 1992;82:341–51.

4. Schulze MM, Hutchings N, Simpson TL. The use of fractal analysis and photometry to estimate the accuracy of bulbar redness grading scales. *Invest Ophthalmol Vis Sci.* 2008;49:1398–406.
5. McMonnies CW, Chapman-Davies A. Assessment of conjunctival hyperemia in contact lens wearers. Part I. *Am J Optom Physiol Opt.* 1987;64:246–50.
6. Institute for Eye Research. IER grading scales. <http://www.siliconehydrogels.org/resources/index.asp>. Accessed 20 July 2007.
7. Efron N. Clinical application of grading scales for contact lens complications. *Optician.* 1997;213:26–35.
8. Schulze M, Jones D, Simpson T. The development of validated bulbar redness grading scales. *Optom Vis Sci.* 2007;84:976–83.
9. Fukushima A, Tomita T. Image analyses of the kinetic changes of conjunctival hyperemia in histamine-induced conjunctivitis in guinea pigs. *Cornea.* 2009;28:694–8.
10. Fukushima A, Tomita T. Image analyses of conjunctival hyperemia in guinea pig allergic conjunctivitis. *Graefes Arch Clin Exp Ophthalmol.* 2009;247:1571–2.
11. Karperien A. FracLac for ImageJ—FracLac advanced user's manual. <http://rsb.info.nih.gov/ij/plugins/fracLac/fracLac-manual.pdf>. Accessed 21 July 2007.
12. Wolffsohn JS. Incremental nature of anterior eye grading scales determined by objective image analysis. *Br J Ophthalmol.* 2004;88:1434–8.
13. Fieguth P, Simpson TL. Automated measurement of bulbar redness. *Invest Ophthalmol Vis Sci.* 2002;43:340–7.
14. Owen CG, Fitzke FW, Woodward EG. A new computer assisted objective method for quantifying vascular changes of the bulbar conjunctivae. *Ophthalm Physiol Opt.* 1996;16:430–7.
15. Papas EB. Key factors in the subjective and objective assessment of conjunctival erythema. *Invest Ophthalmol Vis Sci.* 2000;41:687–91.
16. Chen PCY, Kovalcheck SW, Zweifach BW. Analysis of microvascular network in bulbar conjunctiva by image processing. *Int J Microcirc Clin Exp.* 1987;6:245–55.
17. Guillon M, Shah D. Objective measurement of contact-lens induced conjunctival redness. *Optom Vis Sci.* 1996;73:596–605.
18. Villumsen J, Ringquist J, Alm A. Image analysis of conjunctival hyperaemia: a personal computer based system. *Acta Ophthalmol.* 1991;69:536–9.
19. Maldonado MJ, Arnau V, Martínez-Costa R, Navea A, Mico FM, Cisneros AL, et al. Reproducibility of digital image analysis for measuring corneal haze after myopic photorefractive keratectomy. *Am J Ophthalmol.* 1997;123:31–41.
20. Willingham FF, Cohen KL, Coggins JM, Tripoli NK, Ogle JW, Goldstein GM. Automatic quantitative measurement of ocular hyperaemia. *Curr Eye Res.* 1995;14:1101–8.
21. Horak F, Berger U, Menapace R, Schuster N. Quantification of conjunctival vascular reaction by digital imaging. *J Allergy Clin Immunol.* 1996;98:495–500.
22. Peterson RC, Wolffsohn JS. Sensitivity and reliability of objective image analysis compared to subjective grading of bulbar hyperaemia. *Br J Ophthalmol.* 2007;91:1464–6.